Journal of Physiology (2002), **545.1**, *pp.* 65–79
DOI: 10.1113/jphysiol.2002.025502

www.jphysiol.org

Subcellular Ca^{2+} alternans represents a novel mechanism for the generation of arrhythmogenic Ca^{2+} waves in cat atrial myocytes

Jens Kockskämper and Lothar A. Blatter

Department of Physiology, Stritch School of Medicine, Loyola University Chicago, 2160 South First Avenue, Maywood, IL 60153, USA

Ca^{2+} alternans is a potentially arrhythmogenic beat-to-beat alternation of the amplitude of the action potential-induced $[Ca^{2+}]_i$ transient in cardiac myocytes. Despite its pathophysiological significance the cellular mechanisms underlying Ca^{2+} alternans are poorly understood. Recent evidence, however, points to the modulation of Ca^{2+}-induced Ca^{2+} release (CICR) from the sarcoplasmic reticulum (SR) by localized alterations in energy metabolism as an important determinant of Ca^{2+} alternans. We therefore studied the subcellular properties of Ca^{2+} alternans in field-stimulated cat atrial myocytes employing fast two-dimensional fluorescence confocal microscopy. Ca^{2+} alternans was elicited by an increase in stimulation frequency or by metabolic interventions targeting glycolysis. Marked subcellular variations in the time of onset, the magnitude, and the phase of alternans were observed. Longitudinal and transverse gradients of Ca^{2+} alternans were found as well as neighbouring subcellular regions alternating out-of-phase. Moreover, focal inhibition of glycolysis resulted in spatially restricted Ca^{2+} alternans. When two adjacent regions within a myocyte alternated out-of-phase, steep $[Ca^{2+}]_i$ gradients developed at their border giving rise to delayed propagating Ca^{2+} waves. The results demonstrate that Ca^{2+} alternans is a subcellular phenomenon caused by modulation of SR Ca^{2+} release, which is mediated, at least in part, by local inhibition of energy metabolism. The generation of arrhythmogenic Ca^{2+} waves by subcellular variations in the phase of Ca^{2+} alternans represents a novel mechanism for the development of atrial disrhythmias.

(Resubmitted 29 May 2002; accepted after revision 5 September 2002; first published online 11 October 2002)
Corresponding author L. A. Blatter: Department of Physiology, Stritch School of Medicine, Loyola University Chicago, 2160 South First Avenue, Maywood, IL 60153, USA. Email: lblatte@lumc.edu

Atrial fibrillation (AF) is characterized by an atrial rate of typically > 400 per minute. It is the most common sustained cardiac arrhythmia affecting millions of people in Europe and the United States alone. Two major complications are associated with AF: (1) impairment of cardiac function and (2) thromboembolism (Nattel *et al.* 2000; Nattel, 2002). Thrombus formation during AF occurs predominantly in the left atrial appendage due to reduced contractility of the atria and associated stasis (Hart & Halperin, 2001). Because of thrombus formation, patients with AF have an increased risk for stroke, which is the most significant factor contributing to morbidity and mortality associated with this type of arrhythmia (Levy, 1998). Recent years have seen considerable progress in unravelling the mechanisms underlying AF, in particular the ionic remodelling that takes place during the course of the disease (Nattel *et al.* 2000; Nattel, 2002). Much less, however, is known about factors causing the onset of fibrillation. A possible mechanism leading to AF is the occurrence of spontaneous sarcoplasmic reticulum (SR) Ca^{2+} release and intracellular Ca^{2+} waves. Ca^{2+} waves are considered arrhythmogenic and are typically observed under conditions of elevated SR Ca^{2+} load (Stern *et al.* 1988; Berlin *et al.* 1989; Wier & Blatter, 1991; Trafford *et al.* 1993, 1995; Cheng *et al.* 1996; Cordeiro *et al.* 2001). A recent study on atrial myocytes from patients undergoing cardiac surgery has linked the pre-operative density of L-type Ca^{2+} current (I_{Ca}) to the occurrence of post-operative AF with a higher I_{Ca} density increasing the likelihood of AF (van Wagoner *et al.* 1999). Moreover, administration of verapamil, an L-type Ca^{2+} channel antagonist, before the onset of AF has been shown to reduce or prevent the ionic remodelling associated with the arrhythmia (Daoud *et al.* 1997; Tieleman *et al.* 1997). Thus, I_{Ca} appears to be an important determinant of the initiation and the maintenance of AF. Presumably, a higher density of I_{Ca} promotes Ca^{2+} overload, which may generate arrhythmogenic Ca^{2+} waves (to initiate AF) and alter gene expression (to induce the remodelling).

Ca^{2+} alternans is a potentially arrhythmogenic abnormality of cardiac Ca^{2+} signalling. It is characterized by alternating large and small amplitude $[Ca^{2+}]_i$ transients. Ca^{2+} alternans underlies electromechanical alternans, a beat-to-beat alternation of action potential duration and contraction

amplitude of cardiac myocytes (Wohlfart, 1982; for review see Euler, 1999). In the electrocardiogram, alternans of (ventricular) action potential duration becomes manifest as alternans of the T-wave configuration. T-wave alternans has been linked to ventricular fibrillation and sudden cardiac death under various conditions including acute myocardial ischaemia (Smith *et al.* 1988; Verrier & Nearing, 1994) and long QT syndrome (Shimizu & Antzelevitch, 1999). It is due to a dispersion of repolarization between different regions of the heart. If sufficient in magnitude the spatial repolarization gradients created during alternans can lead to unidirectional block and thus provide the substrate for re-entrant arrhythmias (Pastore *et al.* 1999). Despite its pathophysiological and clinical significance, the cellular mechanisms underlying the various forms of cardiac alternans are poorly understood. The key to their understanding, however, lies in the regulation of SR Ca^{2+} release since interventions known to inhibit this process abolish electromechanical alternans in isolated myocytes (Rubenstein & Lipsius, 1995) as well as in multicellular cardiac preparations (Shimizu & Antzelevitch, 1999). Furthermore, Ca^{2+} alternans can be observed during action potential clamp (Chudin *et al.* 1999), i.e. in the absence of electrical alternations. In other words, mechanical and electrical alternans appear to be secondary to Ca^{2+} alternans.

Cardiac alternans has been studied mainly at the level of the whole heart or in ventricular preparations, including isolated ventricular myocytes. Much less attention has been paid to atrial alternans, although, as pointed out above, atrial arrhythmias represent a major health problem and occur far more often than ventricular arrhythmias. A recent study from our laboratory compared alternans in atrial and ventricular myocytes from the cat heart (Hüser *et al.* 2000). Evidence was presented for both cell types suggesting that glycolysis and SR Ca^{2+} release are functionally coupled. The data supported the hypothesis that SR Ca^{2+} release is sensitive to metabolic changes in the microenvironment of the ryanodine receptor Ca^{2+} release channel (RyR) and that inhibition of glycolytic flux can cause Ca^{2+} alternans via impairment of SR Ca^{2+} release. If this hypothesis is correct, Ca^{2+} alternans would be expected to display subcellular variations depending on local energy metabolism. Therefore, the aim of the current study was to investigate the subcellular features of cardiac Ca^{2+} alternans during metabolic interventions. Atrial myocytes were used as a model system for two reasons. First, our previous results indicated that atrial Ca^{2+} alternans is spatially much less homogeneous than ventricular Ca^{2+} alternans (Hüser *et al.* 2000). Second, a detailed investigation of abnormalities in atrial Ca^{2+} signalling might reveal novel insights into the generation of atrial arrhythmias, in particular the initiation of AF. The results revealed remarkable regional differences in Ca^{2+} alternans within single atrial myocytes that were linked to local metabolism. When neighbouring subcellular regions alternated out-of-phase, propagating Ca^{2+} waves developed at the border of the two regions. The findings establish a direct link between Ca^{2+} alternans and Ca^{2+} waves and support the notion that SR Ca^{2+} release is tightly coupled to local metabolism. They demonstrate, for the first time, that subcellular Ca^{2+} alternans can generate potentially arrhythmogenic Ca^{2+} waves and thus might represent a substrate for atrial arrhythmias.

METHODS

Experimental procedure

The procedure for cell isolation was in accordance with institutional guidelines for animal care. Myocytes from the left atrium of the cat heart were isolated as described previously (Wu *et al.* 1991). Briefly, cats were anaesthetized with pentobarbital sodium (50 mg kg^{-1} I.P.). Following thoracotomy, hearts were quickly excised, mounted on a Langendorff apparatus, and retrogradely perfused with oxygenated collagenase-containing solution at 37 °C.

Cells were plated on glass coverslips and loaded with fluo-4 (Molecular Probes, Eugene, OR, USA) by 30 min exposure to Tyrode solution (mM: 140 NaCl, 5 KCl, 2 $CaCl_2$, 1 $MgCl_2$, 10 glucose, and 10 Hepes; pH 7.35 with NaOH) containing 45 μM of the acetoxymethyl ester of the Ca^{2+} indicator. A coverslip with dye-loaded myocytes was transferred to the stage of an inverted microscope (Nikon Diaphot) equipped with a ×60 water-immersion objective lens (Nikon CF Plan Apochromat, NA = 1.2). Cells were superfused with Tyrode solution and ⩾15 min were allowed for de-esterification of the indicator. Myocytes were electrically stimulated through a pair of platinum electrodes at a frequency of 0.5–0.7 Hz. Focal application of various modified Tyrode solutions was performed through pressure ejection from a glass pipette (~1–2 μm tip diameter) positioned close to the sarcolemma. Iodoacetate (0.2 mM) was added to normal glucose-containing Tyrode solution. Glucose was omitted from Tyrode solutions containing sodium pyruvate (10 mM) plus sodium β-hydroxybutyrate (10 mM) or sucrose (40 mM). All experiments were performed at room temperature (22–25 °C).

Ca^{2+} imaging

Two-dimensional confocal Ca^{2+} imaging was performed using an intensified CCD camera (Stanford Photonics, Palo Alto, CA, USA) coupled to a Nipkow dual-disc laser scanning unit (CSU10, Yokogawa Electric Co., Tokyo, Japan), as described previously (Kockskämper *et al.* 2001). Fluo-4 was excited by the 488 nm line of an argon ion laser (532-A-A04, Omnichrome, Chino, CA, USA). The emitted fluorescence was collected at wavelengths > 515 nm. Interlaced images (512 pixels × 480 pixels) were acquired and digitized at video rate (30 Hz). Pixel size was 0.33 μm (horizontal) × 0.27 μm (vertical). Changes of $[Ca^{2+}]_i$ are expressed as changes of normalized fluorescence (F/F_0). F_0 was obtained by averaging five background-subtracted full-frame images during diastole. Images were de-interlaced resulting in a temporal resolution of 60 Hz. Fluo-4 fluorescence or F/F_0 images are shown.

Ca^{2+} alternans

Alternans of the $[Ca^{2+}]_i$ transient amplitude (Ca^{2+} alternans) was elicited by an increase in stimulation frequency from 0.5 to 1.0 Hz, or by application of pyruvate, pyruvate plus β-hydroxybutyrate, or iodoacetate at constant stimulation frequency (0.5–0.7 Hz).

The magnitude of Ca^{2+} alternans was quantified as the alternans ratio (AR). The AR was defined as $1 - S/L$, where S/L is the ratio of the small amplitude $[Ca^{2+}]_i$ transient (S) to the large amplitude $[Ca^{2+}]_i$ transient (L) during a pair of alternating $[Ca^{2+}]_i$ transients (Wu & Clusin, 1997). Thus, the AR had values between 1 and 0, with AR = 0 indicating no alternans and AR = 1 indicating the highest possible degree of alternans, with only every other stimulation resulting in a measurable $[Ca^{2+}]_i$ transient.

Statistics

Data are presented as means ± standard error of the mean (S.E.M.) obtained from n different cells. Statistical differences between data sets were evaluated by Student's t test.

RESULTS

Subcellular Ca^{2+} alternans in cat atrial myocytes

Figure 1 illustrates subcellular $[Ca^{2+}]_i$ transients of single atrial myocytes (upper panels) subjected to three different protocols. Under control conditions (Fig. 1*A*) subcellular $[Ca^{2+}]_i$ transients from various regions within the cell (*a–d*) displayed similar amplitudes that remained constant throughout the recording. An increase in stimulation frequency from 0.5 to 1.0 Hz, however, led to Ca^{2+} alternans, i.e. alternating large and small amplitude $[Ca^{2+}]_i$ transients (Fig. 1*B*). Alternans started immediately upon the change in stimulation frequency and its magnitude varied within the cell. It was largest in the upper part (*a* and *b*) and much less pronounced in the lower part of the myocyte (*c*), indicating a longitudinal gradient of Ca^{2+} alternans within the cell. Alternans was also caused by replacing glucose with pyruvate (Fig. 1*C*; see also Hüser *et al.* 2000). In contrast to pacing-induced alternans (Fig. 1*B*), pyruvate-mediated Ca^{2+} alternans took much longer to develop, usually tens of seconds, suggesting the involvement of a metabolic process (Hüser *et al.* 2000). In the presence of pyruvate, alternans patterns in different regions of the cell were also variable. For example, region *b* exhibited an increasingly high degree of alternans. By contrast, alternans in region *a* developed much later and to a lesser degree and region *c* did not display any alternans at all. Thus, the time of onset and the magnitude of alternans exhibited marked subcellular variations.

Figure 2 shows the detailed spatio-temporal characteristics of the two shaded pairs of $[Ca^{2+}]_i$ transients of the cell displayed in Fig. 1*C*. Figure 2*A* illustrates fluo-4 fluorescence images of the atrial myocyte obtained immediately before (*a*, 0 ms), during the upstroke (*b–e*, 17–83 ms), and during the declining phase (*f–h*, 217–750 ms) of the $[Ca^{2+}]_i$ transients. The first pair of transients (left panel) was recorded at the beginning of the experiment under control conditions, whereas the second pair (right panel) was recorded during pyruvate-induced Ca^{2+} alternans. In all

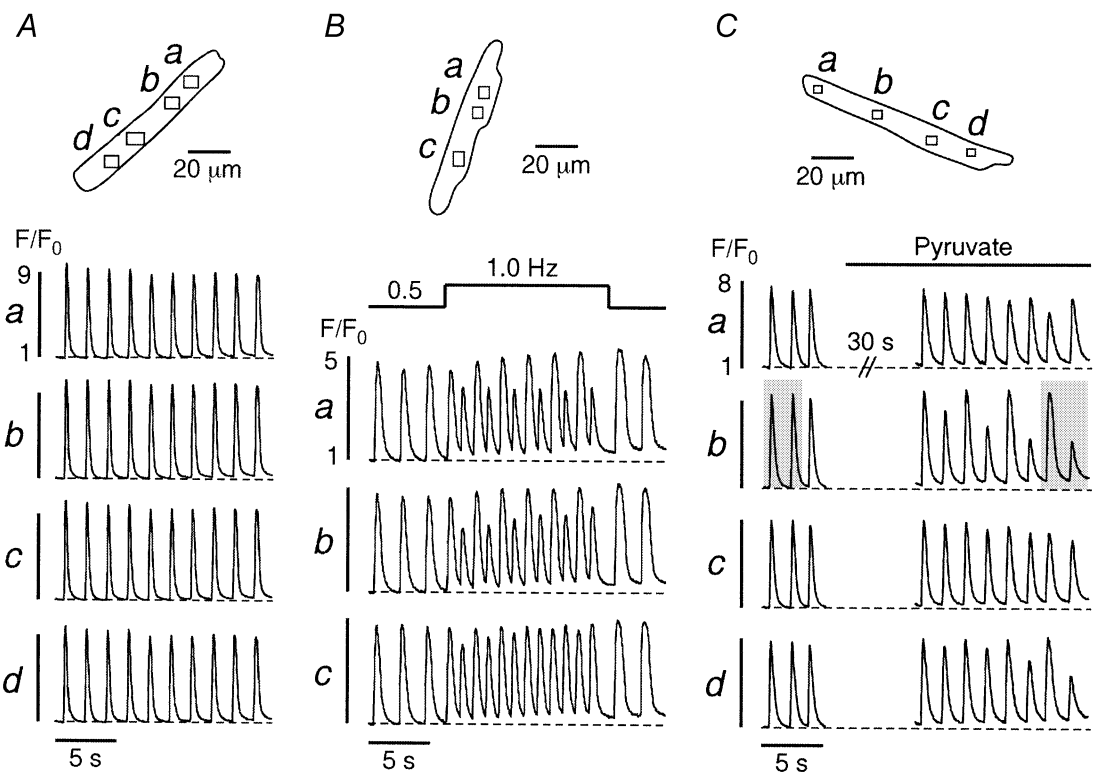

Figure 1. Induction of Ca^{2+} alternans

A, under control conditions (glucose-containing Tyrode solution) various regions (*a–d*) of an atrial myocyte exhibit uniform $[Ca^{2+}]_i$ transients. An increase in stimulation frequency from 0.5 to 1.0 Hz (*B*) or application of pyruvate-containing (10 mM) solution (*C*) elicit Ca^{2+} alternans. Stimulation frequency in *A* and *C*, 0.6 Hz. The shaded areas in *C* mark the $[Ca^{2+}]_i$ transients shown in more detail in Fig. 2.

four cases resting fluorescence (panels *a*) was distributed relatively homogeneously throughout the cell suggesting that there was no major compartmentalization of the dye. Electrical stimulation occurred between 0 and 17 ms and elicited increases of $[Ca^{2+}]_i$. Comparison of the images of the first two $[Ca^{2+}]_i$ transients (left panel, control) revealed virtually no differences. In both cases $[Ca^{2+}]_i$ increased in the subsarcolemmal regions first, forming a ring of elevated $[Ca^{2+}]_i$ (*b* and *c*), before spreading to the centre of the myocyte (*d–f*) and finally declining towards resting values

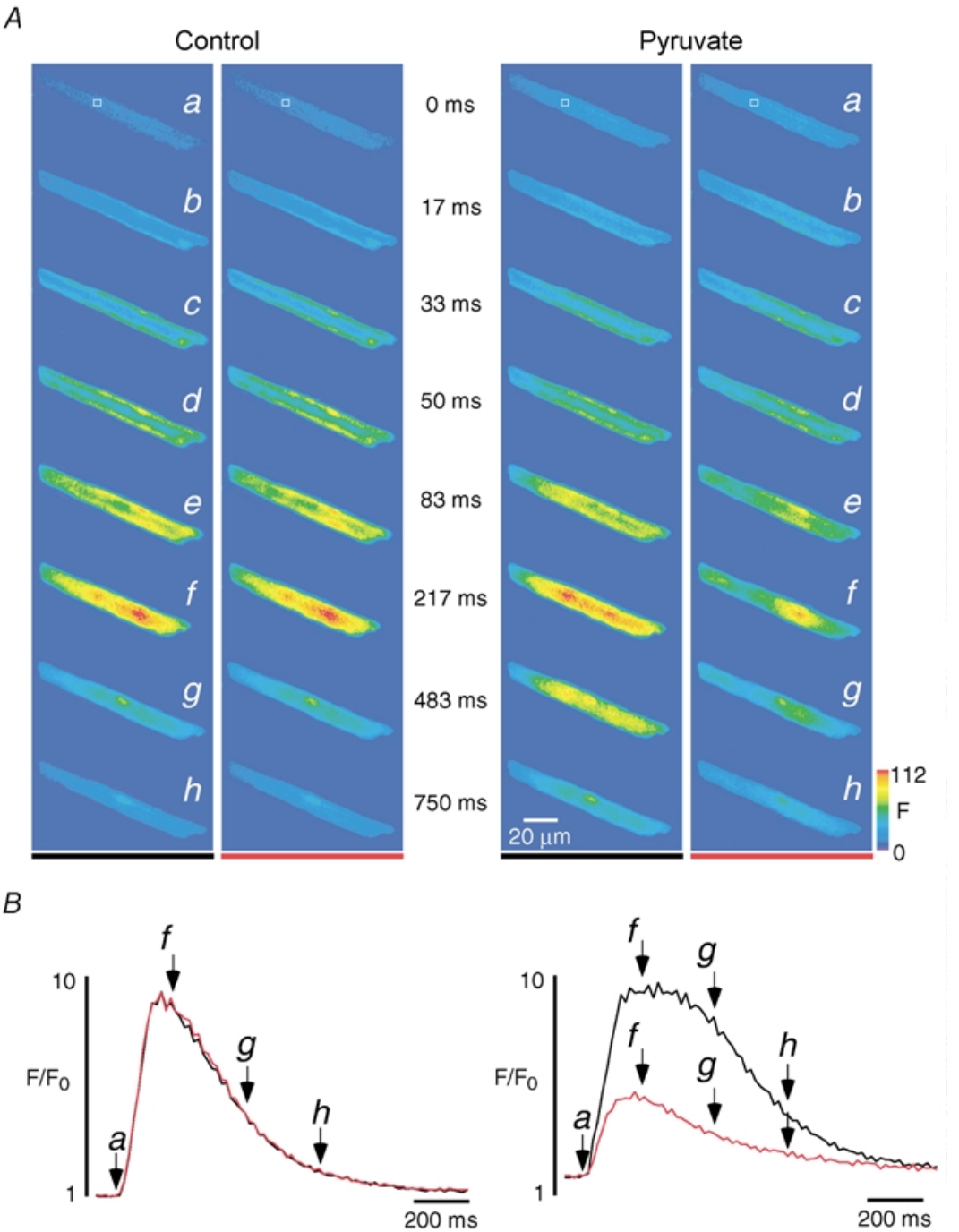

Figure 2. Spatio-temporal characteristics of $[Ca^{2+}]_i$ transients before and during Ca^{2+} alternans

A, fluo-4 fluorescence images of two pairs of $[Ca^{2+}]_i$ transients recorded before (left) and during (right) pyruvate-induced Ca^{2+} alternans. The images in row *a* and marked 0 ms show $[Ca^{2+}]_i$ at rest and refer to the video fields immediately preceding the first observable changes of $[Ca^{2+}]_i$. *B*, local $[Ca^{2+}]_i$ transients recorded from the region of interest marked by the square in *Aa* and shown on an expanded time scale. The two successive $[Ca^{2+}]_i$ transients under control conditions (left; black before red) show identical amplitudes and kinetics. In contrast, the amplitude and kinetics of the pair of $[Ca^{2+}]_i$ transients during alternans induced by pyruvate (10 mM) both vary significantly (right, black before red). The letters and arrows refer to the images in *A*.

(*g* and *h*). Figure 2*B* (left panel) shows the $[Ca^{2+}]_i$ transients of the region depicted in Fig. 2*Aa* (same as region *b* in Fig. 1*C*). The black trace represents the first $[Ca^{2+}]_i$ transient and the red trace the second $[Ca^{2+}]_i$ transient. Letters *a*, *f*, *g* and *h* correspond to the images in Fig. 2*A*. The two control $[Ca^{2+}]_i$ transients were almost perfectly identical indicating that under control conditions action potential-induced $[Ca^{2+}]_i$ signals exhibited reproducible spatio-temporal characteristics. By contrast, the pair of $[Ca^{2+}]_i$ transients recorded during Ca^{2+} alternans (Fig. 2*B*, right panel) showed substantial differences. The first, large amplitude $[Ca^{2+}]_i$ transient (black trace) exhibited a relatively homogeneous $[Ca^{2+}]_i$ increase. Its amplitude was similar to the amplitude under control conditions. Its kinetics, however, were somewhat slowed, in particular at the subcellular region chosen for analysis. The peak was considerably broader than under control conditions (compare images at 483 ms in Fig. 2*A*) suggesting that the kinetics of Ca^{2+} release and/or removal were altered. The second, low amplitude $[Ca^{2+}]_i$ transient, on the other hand, exhibited an inhomogeneous $[Ca^{2+}]_i$ increase. Whereas most regions (including the one chosen for analysis, red trace) showed only small elevations of $[Ca^{2+}]_i$, an area in the lower right part of the cell displayed a large increase in $[Ca^{2+}]_i$ (region *c* in Fig. 1*C*). In addition, the small amplitude $[Ca^{2+}]_i$ transient was shorter in duration (duration at half-maximum amplitude) and its kinetics differed from the preceding large amplitude $[Ca^{2+}]_i$ transient (Fig. 2*B*). Thus, during Ca^{2+} alternans the spatio-temporal characteristics of alternating $[Ca^{2+}]_i$ transients were highly variable.

Subcellular Ca^{2+} alternans can be graded or out-of-phase

Figure 3 illustrates that an increase in stimulation frequency can cause a transverse gradient of Ca^{2+} alternans. At 0.5 Hz various subcellular regions of an atrial myocyte (Fig. 3*A*, left, *a*–*e*) exhibited uniform $[Ca^{2+}]_i$ transients (Fig. 3*Ba*–*e*).

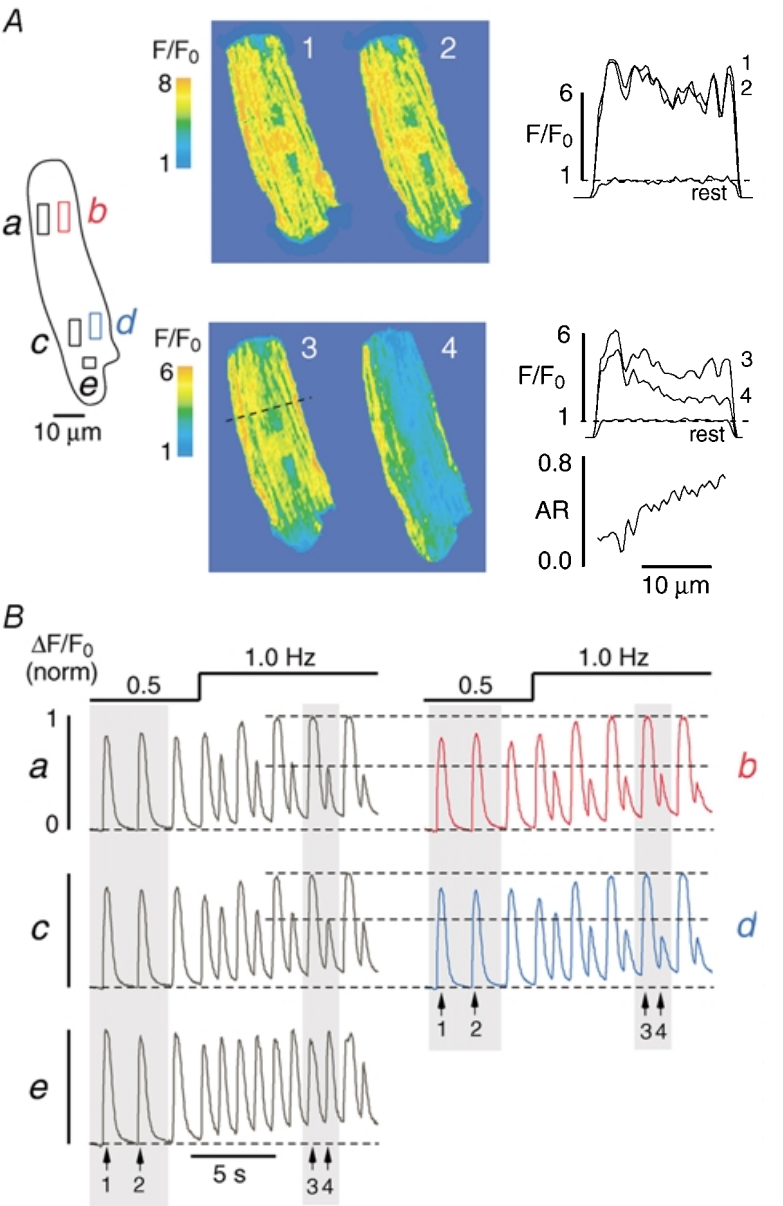

Figure 3. Transverse gradient of Ca^{2+} alternans

$[Ca^{2+}]_i$ (F/F_0) images (*A*) and normalized subcellular $[Ca^{2+}]_i$ transients (*B*) from various regions of interest (*a*–*e*) recorded from an atrial myocyte under control conditions and during pacing-induced Ca^{2+} alternans. The increase in stimulation frequency from 0.5 to 1.0 Hz induces large Ca^{2+} alternans at sites *a*–*d*, but only small alternans at site *e*. The $[Ca^{2+}]_i$ images (1–4) in *A* were taken during the shaded $[Ca^{2+}]_i$ transients in *B* at the times indicated by the arrows. Profile plots (F/F_0) along the dashed line recorded under control conditions (1, 2) and during Ca^{2+} alternans (3, 4) are illustrated on the right of panel *A*. 'Rest' denotes a profile plot obtained from the same line under resting conditions. The alternans ratio (AR), i.e. 1 minus the amplitude of profile 4 divided by profile 3, is shown on the lower right (*A*). It reveals a transverse gradient of Ca^{2+} alternans.

Images of the cell taken at the peak of the first two transients (arrows 1 and 2 in Fig. 3*B*) are shown in Fig. 3*A* (top). They revealed the typical atrial pattern of a few intracellular rows of elevated $[Ca^{2+}]_i$ and somewhat higher subsarcolemmal $[Ca^{2+}]$ as compared with the cell centre (Kockskämper *et al.* 2001). The $[Ca^{2+}]_i$ (F/F_0) profiles along the dashed line perpendicular to the longitudinal axis of the myocyte (top right) show that this pattern was fairly symmetrical across the cell and that the amplitudes of the two $[Ca^{2+}]_i$ transients were almost identical. Consequently the AR had values close to 0 (< 0.15; not shown).

When the stimulation frequency was increased to 1.0 Hz, all regions (except for region *e*) displayed large Ca^{2+} alternans (Fig. 3*B*). Analysis of the $[Ca^{2+}]_i$ transients from neighbouring regions revealed that alternans was much more pronounced on the right side (*b* and *d*) as compared with the left side of the cell (*a* and *c*). This is shown in detail in Fig. 3*A* (bottom). Images of the cell obtained during a pair of large and small amplitude $[Ca^{2+}]_i$ transients (arrows 3 and 4 in Fig. 3*B*) are presented. The amplitude of the large $[Ca^{2+}]_i$ increase was relatively symmetrical across the cell, similar to control conditions. By contrast, the amplitude of the small $[Ca^{2+}]_i$ transient decreased from left to right. The

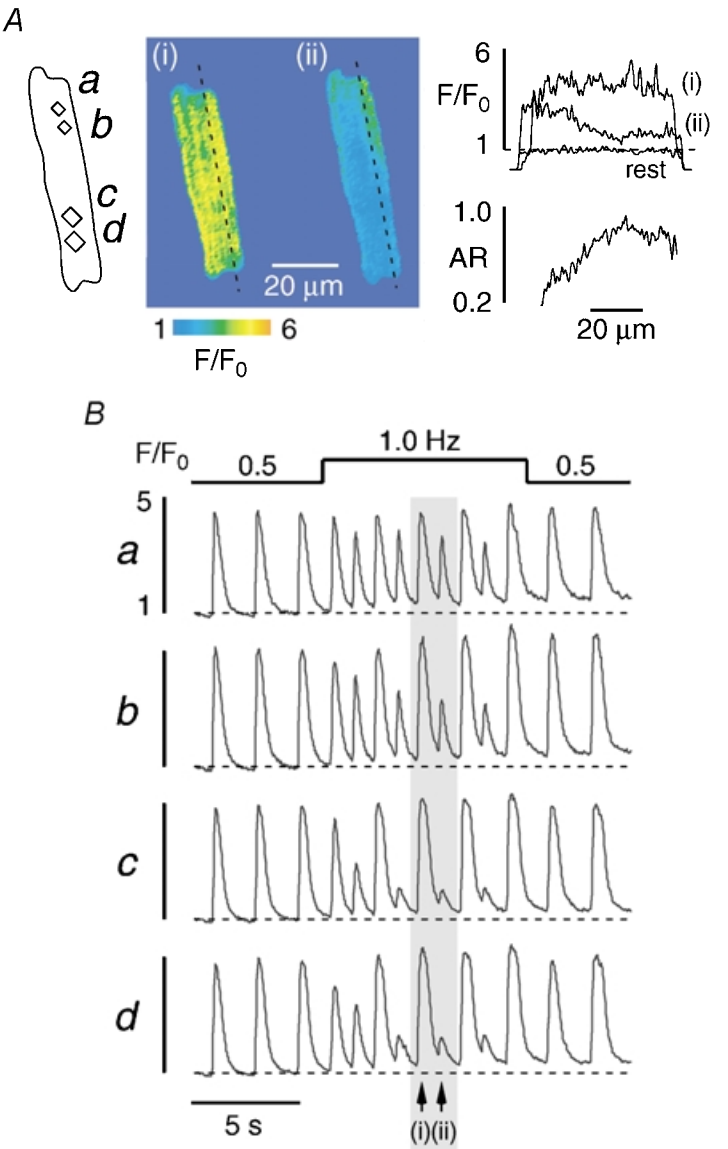

Figure 4. Longitudinal gradient of Ca^{2+} alternans

$[Ca^{2+}]_i$ (F/F_0) images (*A*) and subcellular $[Ca^{2+}]_i$ transients from various regions (*a–d*) of an atrial cell (*B*). The increase in stimulation frequency from 0.5 to 1.0 Hz results in Ca^{2+} alternans that gradually increases from region *a* to *d*. The two images of the myocyte shown in *A* were taken during the shaded $[Ca^{2+}]_i$ transients in *B* at the times indicated by the arrows. Profile plots (F/F_0) along the dashed line are illustrated on the upper right (*A*) together with a profile plot obtained under resting conditions ('rest'). The AR (*A*, lower right) reveals a longitudinal gradient of Ca^{2+} alternans in the upper part of the cell.

$[Ca^{2+}]_i$ (F/F_0) profiles along the dashed line confirm this observation (Fig. 3*A*, bottom right). The difference in $[Ca^{2+}]_i$ increased from left to right, resulting in a steep transverse gradient of Ca^{2+} alternans. Hence, the AR increased sharply and almost linearly from 0.2 on the left side to ~0.7 on the right side of the cell.

In another myocyte (Fig. 4*A*), increasing the stimulation frequency from 0.5 to 1.0 Hz caused a longitudinal gradient of Ca^{2+} alternans. $[Ca^{2+}]_i$ transients from various regions (*a–d*) within the cell show that alternans during 1.0 Hz stimulation was more pronounced in the lower half (*c* and *d*) than in the upper half (*a* and *b*) of the cell (Fig. 4*B*). Images recorded during a large (i) and a small (ii) amplitude $[Ca^{2+}]_i$ transient (shaded area in Fig. 4*B*) are depicted in Fig. 4*A* (middle panel). The homogeneous $[Ca^{2+}]_i$ increase during the large transient contrasted with the inhomogeneous $[Ca^{2+}]_i$ signal of the small transient. During the small $[Ca^{2+}]_i$ transient significant Ca^{2+} release was evident only in the upper part of the myocyte. Figure 4*A* (right) illustrates the two profile plots along the dashed line parallel to the longitudinal axis of the cell (top) and the resulting AR (bottom). The AR exhibited an increase from 0.2 to ~0.8 in the upper half of the myocyte, thus revealing a steep longitudinal gradient of Ca^{2+} alternans in this part of the cell. By contrast, the lower half of the myocyte displayed an almost constant AR of ~0.7 and thus little variation in the degree of alternans.

Yet another pattern of subcellular Ca^{2+} alternans is presented in Fig. 5. In this example alternans was induced by application of pyruvate. The subcellular regions chosen for analysis are shown in Fig. 5*A* (top panel, left, *a–d*), together with a series of fluorescence images of the rising phase of a $[Ca^{2+}]_i$ transient obtained under control conditions (first transient (i) in Fig. 5*B* marked by the arrow). Each of these regions exhibited uniform $[Ca^{2+}]_i$ transients in Tyrode solution containing glucose (10 mM; Fig. 5*Ba–d*). About 45 s after switching to pyruvate (10 mM) Ca^{2+} alternans was observed in the lower part of the cell only (Fig. 5*Bd*). Within the next few beats, however, it spread to the upper part of the cell such that the whole myocyte displayed Ca^{2+} alternans. Remarkably, the upper and the lower parts of the cell were alternating out-of-phase (indicated by the arrows in Fig. 5*B*, right panel). The large amplitude $[Ca^{2+}]_i$ transient in the lower part (ii) coincided with the small amplitude $[Ca^{2+}]_i$ transient in the upper part of the cell and vice versa (iii), a pattern that is obvious in the corresponding two series of fluorescence images in Fig. 5*A* (middle and bottom panel). Thus, subcellular Ca^{2+} alternans was characterized by large gradients, either transverse (Fig. 3) or longitudinal (Fig. 4), and neighbouring regions alternating out-of-phase (Fig. 5). Table 1 summarizes these findings. Overall, 29 cells were studied, 15 with pacing-induced Ca^{2+} alternans and 14 with pyruvate-induced Ca^{2+} alternans. Only eight cells (18 %) exhibited spatially homogeneous alternans. Subcellularly inhomogeneous Ca^{2+} alternans was observed in the majority of myocytes (21/29 cells, 72 %). It was found in 64 % of the pyruvate-treated cells (9/14 cells) and in 80 % of the cells in which alternans was evoked by an increase in stimulation frequency (12/15 cells). In many cases, the various forms of subcellular Ca^{2+} alternans occurred in a single cell during a single alternans episode (e.g. Figs 1*C* and 5). Twenty myocytes displayed longitudinal gradients of Ca^{2+} alternans whereas only three cells exhibited transverse alternans gradients. Ca^{2+} alternans with neighbouring subcellular regions alternating out-of-phase was observed in 12 cells. In each case, the average maximum AR ($AR_{maximum}$) amounted to ~0.65 as compared with negligible values of ~0.05 before pacing or pyruvate treatment ($AR_{control}$ in Table 1). The longitudinal and transverse alternans gradients were large. On average, the difference of the AR between the subcellular regions displaying the highest and the lowest degree of Ca^{2+} alternans ($\Delta AR_{gradient}$) was 0.37 ± 0.03 (n = 20). Both pacing- and pyruvate-induced Ca^{2+} alternans were reversible. After either withdrawal of pyruvate or a return to baseline stimulation frequency (0.5 Hz), the AR amounted to 0.05 ± 0.02 (n = 10). Furthermore, the amplitude of the $[Ca^{2+}]_i$ transient returned to 90 ± 3 % of the pre-alternans control (n = 10). No systematic differences in these numbers were found between pacing-induced and pyruvate-induced Ca^{2+} alternans.

Table 1. Summary of subcellular Ca^{2+} alternans characteristics

Subcellular Ca^{2+} alternans	Number of cells	$AR_{control}$	$AR_{maximum}$	$\Delta AR_{gradient}$
All forms	29	0.05 ± 0.01	0.65 ± 0.03	—
Gradients	20	0.04 ± 0.01	0.64 ± 0.03	0.37 ± 0.03
Out-of-phase	12	0.05 ± 0.02	0.62 ± 0.03	—
Homogeneous	8	0.07 ± 0.04	0.68 ± 0.09	—

Ca^{2+} alternans was induced by pacing (15 cells) or by exposure to pyruvate (14 cells). AR, alternans ratio. $AR_{control}$, ratio of the amplitude of two successive $[Ca^{2+}]_i$ transients before induction of alternans. $AR_{maximum}$, maximum subcellular AR. $\Delta AR_{gradient}$, difference of the AR between the subcellular regions displaying the highest and the lowest degree of Ca^{2+} alternans. Data represent means ± S.E.M.

Focal inhibition of glycolysis causes subcellularly restricted Ca^{2+} alternans

The results presented above revealed substantial regional differences in the time of onset, the magnitude, and the phase of cellular Ca^{2+} alternans, suggesting that the mechanisms causing this phenomenon are regulated on a restricted subcellular level. To further test this hypothesis we focally applied iodoacetate (0.2 mM) or pyruvate (10 mM) plus β-hydroxybutyrate (10 mM; Pyr + βHB) through a pipette to one end of the myocyte, while the remaining part was superfused with glucose-containing

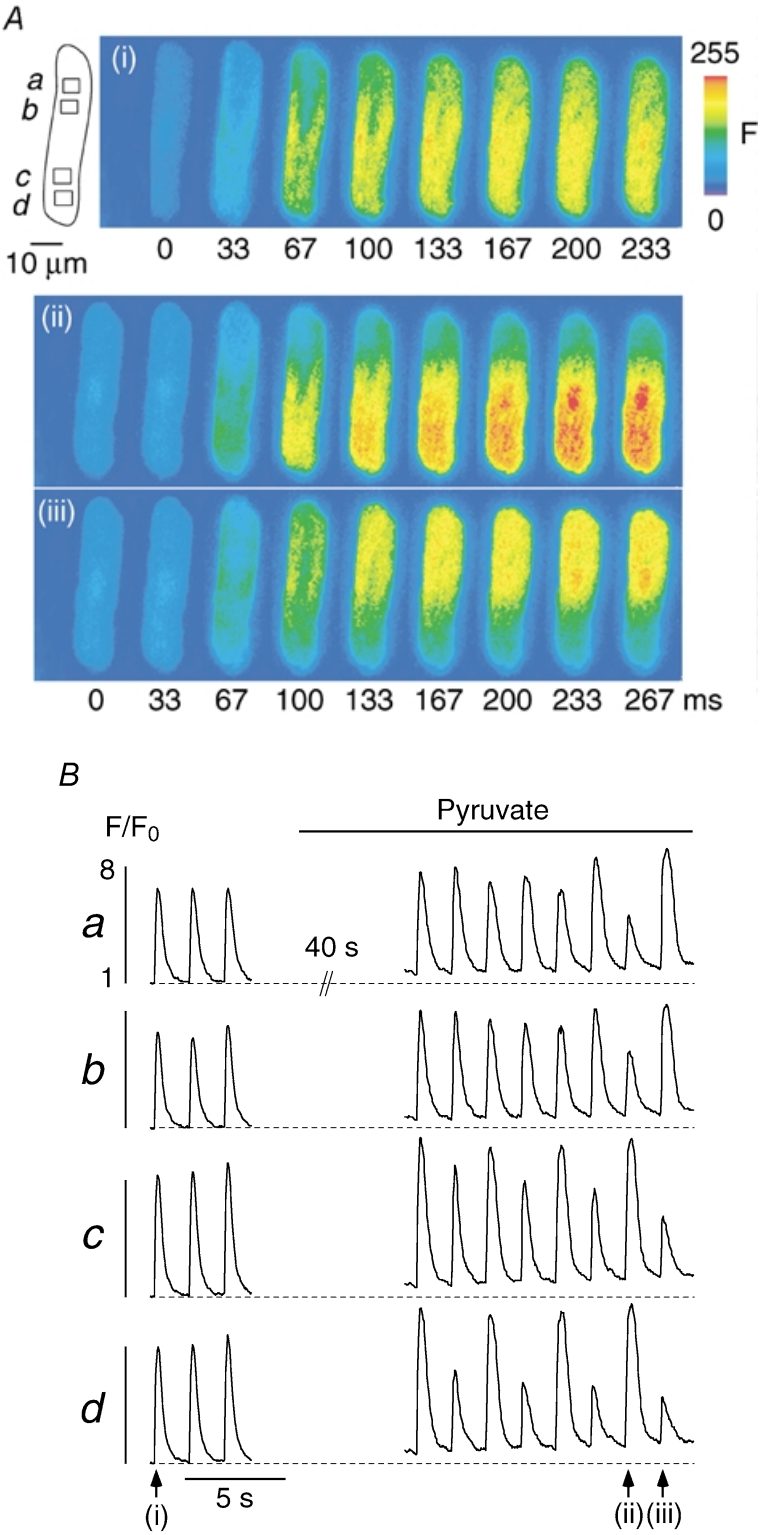

Figure 5. Neighbouring regions within an atrial myocyte alternate out-of-phase

Ca^{2+} alternans was induced by application of pyruvate. *A*, series of fluo-4 fluorescence images recorded under control conditions and during Ca^{2+} alternans. The images illustrate the rising phase of the $[Ca^{2+}]_i$ transients marked by the arrows in *B*. *B*, subcellular $[Ca^{2+}]_i$ transients recorded from the regions marked by the rectangles *a–d* (*A*). $[Ca^{2+}]_i$ images and subcellular $[Ca^{2+}]_i$ transients reveal that the time of onset, the magnitude, and the phase of Ca^{2+} alternans exhibit large subcellular variations and that the upper and the lower half of the cell alternate out-of-phase. Stimulation frequency, 0.6 Hz.

Tyrode solution (Fig. 6*B* and *C*, top panels), thus preventing exposure to the solution ejected from the pipette. The three substances have previously been shown to induce global Ca^{2+} alternans in these cells, presumably through inhibition of glycolysis (Newsholme *et al.* 1962; Hüser *et al.* 2000). To verify the focal nature of application through the glass pipettes we performed control experiments with fluorescein-containing pipette solution (20 μM fluorescein in Tyrode solution). Figure 6*Aa* shows an atrial myocyte and the glass pipette. A large diameter superfusion pipette was positioned to the left of the cell as indicated by the horizontal arrows, placing the cell in the laminar flow of the bulk bath solution. Pressure ejection of the fluorescein-containing pipette solution induced a clearly visible cloud of fluorescence that covered the right side of the myocyte downstream of the laminar superfusion flow but not the left side of the cell. The profile (Fig. 6*Ab*) measured along the dashed line shown in panel *Aa* reveals that fluorescence was maximal directly at and up to ~20 μm downstream of the pipette tip. Immediately upstream of the pipette tip, however, fluorescence declined sharply to 50 % (F_{50}) and 10 % (F_{10}) of its maximum within 6.5 and 15.7 μm, respectively. For comparison, a profile plot along the same line before pressure application of the pipette solution revealed uniform background fluorescence (Fig. 6*Ab*, lower trace). Thus, in the absence of any pressure there was no leakage of the solution from the pipette tip. Together these results confirm that this method was well suited for focal application of the various test solutions designed to induce local Ca^{2+} alternans.

Focal application of iodoacetate caused distinct spatially restricted changes of the $[Ca^{2+}]_i$ transient, including Ca^{2+} alternans (Fig. 6*B*). During iodoacetate treatment two premature beats (i.e. $[Ca^{2+}]_i$ transients triggered by spontaneous action potentials) were observed (arrows under trace *c*). The first one was interpolated between two regular beats whereas the second one was followed by a compensatory pause. Strikingly, during both premature beats $[Ca^{2+}]_i$ transients were greatly diminished near the site of iodoacetate application (*a* and *b*) but much less affected at a distant region (*c*). This suggested that already at this time Ca^{2+} release was impaired in a spatially restricted fashion by local inhibition of glycolysis. About 20 s later, during washout of iodoacetate, Ca^{2+} alternans was evident near the site of iodoacetate application (*a* and *b*) but not at the distant site (*c*). The most pronounced effects were seen at the region closest to the pipette tip (*a*). The alternans pattern of this region (shaded area) is shown on an expanded scale in the bottom panel (Fig. 6*B*). Three of the four $[Ca^{2+}]_i$ transients exhibited two peaks. The first peaks (filled circles) were due to electrical stimulation-induced Ca^{2+} release and showed clear alternans with an average AR of 0.37. By contrast, each of the secondary peaks was the result of a delayed locally restricted Ca^{2+} wave propagating through the upper part of the myocyte (compare Fig. 7).

Similar to iodoacetate, focal application of pyruvate plus β-hydroxybutyrate (Pyr + βHB) also caused spatially restricted Ca^{2+} alternans (Fig. 6*C*). After applying pyruvate and β-hydroxybutyrate together for 20 s (horizontal bar in *a*) $[Ca^{2+}]_i$ transients of alternating large and small amplitudes were observed at the site near the pipette tip (*a*) but not at distant regions (*b*–*d*). The AR of the $[Ca^{2+}]_i$ transients at region *a*, averaged over the last four beats, amounted to 0.45 as compared with an AR of 0.03 at region *d*. In a total of six myocytes, the AR of the sites close to the pipette tip (bottom, □) was 0.52 ± 0.08 and thus significantly larger than the AR at distant sites (■), where no alternans was detected (AR = 0.08 ± 0.01; $n = 6$, $P < 0.01$). Locally restricted Ca^{2+} alternans was observed as soon as two beats after starting focal application of pyruvate and β-hydroxybutyrate. It therefore occurred much faster than the subcellular Ca^{2+} alternans induced by global application of pyruvate alone (Figs 1*C* and 5).

To verify that pressure application by itself did not induce the observed Ca^{2+} alternans, control experiments were conducted in the absence of iodoacetate and pyruvate plus β-hydroxybutyrate. To account for the increased osmolarity of the latter solution, 40 mM sucrose was added to the glucose-free Tyrode solution in these experiments. As shown in Fig. 6*D*, focal application of the sucrose-containing solution did not affect local $[Ca^{2+}]_i$ transients. Ca^{2+} alternans was never observed under these conditions. In three cells subjected to this protocol, ARs at sites near to (□) or far from (■) the pipette tip had identical values of 0.05 ± 0.01, revealing typical small beat-to-beat variability of the $[Ca^{2+}]_i$ transient amplitude under control conditions (see also Table 1).

Subcellular Ca^{2+} alternans leads to propagating Ca^{2+} waves

Under conditions where two neighbouring regions were alternating out-of-phase or, alternatively, one region exhibited large Ca^{2+} alternans whereas an adjacent region did not alternate, subcellular Ca^{2+} alternans could develop into propagating waves of $[Ca^{2+}]_i$. This phenomenon is illustrated in Fig. 7. An atrial myocyte (Fig. 7*A*) was challenged with pyruvate to induce subcellular Ca^{2+} alternans. Local $[Ca^{2+}]_i$ transients from regions in the upper (*a*) and lower (*b*) part of the cell are shown in Fig. 7*B*. In the presence of glucose $[Ca^{2+}]_i$ transients in both regions had identical characteristics and showed no signs of alternans. During pyruvate application, however, pronounced Ca^{2+} alternans was observed in the upper part of the cell (region *a*), whereas the lower part (region *b*) exhibited only a slight reduction in $[Ca^{2+}]_i$ transient amplitude but no alternans. During the fifth alternans beat (shaded area in Fig. 7*B*) this pattern led to the generation of a delayed propagating Ca^{2+} wave, as illustrated in Fig. 7*C* (ii). For comparison fluorescence images of the cell from the first (control) $[Ca^{2+}]_i$ transient are also shown (i). The

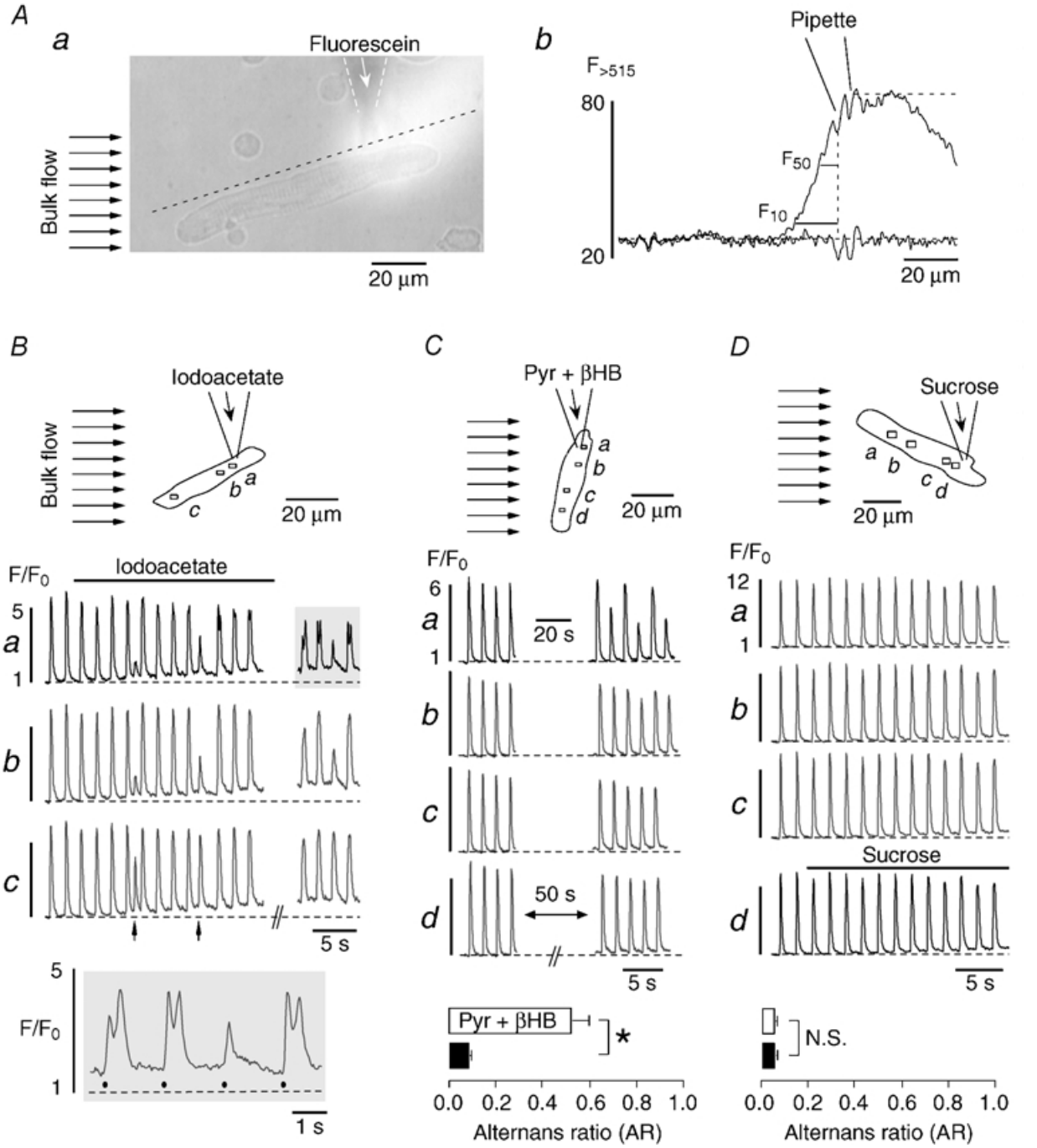

Figure 6. Focal inhibition of glycolysis induces subcellularly restricted Ca^{2+} alternans

A, method for the focal application of inhibitors of glycolysis. A fluorescein-containing (20 μM) Tyrode solution was pressure-ejected from a glass micropipette (*a*). The bulk solution flow in the tissue bath (marked by the arrows to the left) restricted exposure of atrial myocytes to the region downstream of the tip of the pipette. Panel *b* shows fluorescein fluorescence profiles recorded along the dashed line in *Aa* before and during solution ejection from the pipette. Upstream of the pipette fluorescein fluorescence declined sharply to 50 % (F_{50}) and 10 % (F_{10}) of its maximum within 6.5 and 15.7 μm from the tip, respectively. *B* and *C*, focal application of inhibitors of glycolysis. *D*, focal application of sucrose. Atrial myocytes were continuously superfused with glucose-containing Tyrode solution (bulk flow, arrows in top panels). Iodoacetate (*B*), pyruvate plus β-hydroxybutyrate (Pyr + βHB) (*C*), or sucrose (*D*) were focally applied to part of the cells through the pipette. Middle panels (*B–D*): subcellular $[Ca^{2+}]_i$ transients from various regions within the myocytes (*a–d*). The arrows in *Bc* mark spontaneous premature beats. Bottom panels: *B*, selected $[Ca^{2+}]_i$ transients from *Ba* (shaded area) on an extended time scale. Filled circles indicate electrical stimulations. *C* and *D*, average alternans ratio of subcellular regions close to (□) and distant from (■) the pipette tip during exposure to pyruvate plus β-hydroxybutyrate ($n = 6$ cells) and sucrose ($n = 3$ cells). $^*P < 0.01$. N.S., difference statistically not significant. Stimulation frequency in all experiments was 0.6 Hz.

latter exhibited the typical features of an atrial $[Ca^{2+}]_i$ transient, including the ring of elevated $[Ca^{2+}]_i$, followed by the rather homogeneous inward spread of $[Ca^{2+}]_i$. During the alternans transient, however, substantial inhomogeneities of $[Ca^{2+}]_i$ were observed. The lower part of the cell displayed a large $[Ca^{2+}]_i$ increase whereas the upper part showed a much smaller elevation of $[Ca^{2+}]_i$. This pattern led to the development of a steep $[Ca^{2+}]_i$ gradient at the border between these two regions (arrows in images at 217 and 283 ms). After an initial decline of $[Ca^{2+}]_i$ a delayed locally restricted $[Ca^{2+}]_i$ increase occurred directly at this border zone (arrowheads at 550, 583 and 617 ms). It propagated in a wave-like fashion into the upper part of the myocyte (583–950 ms), where only a small $[Ca^{2+}]_i$ increase had been elicited by the electrical stimulation (marked by the filled circle in Fig. 7*B*). This pattern of a small amplitude $[Ca^{2+}]_i$ transient followed by a propagating Ca^{2+} wave translated into a $[Ca^{2+}]_i$ signal with

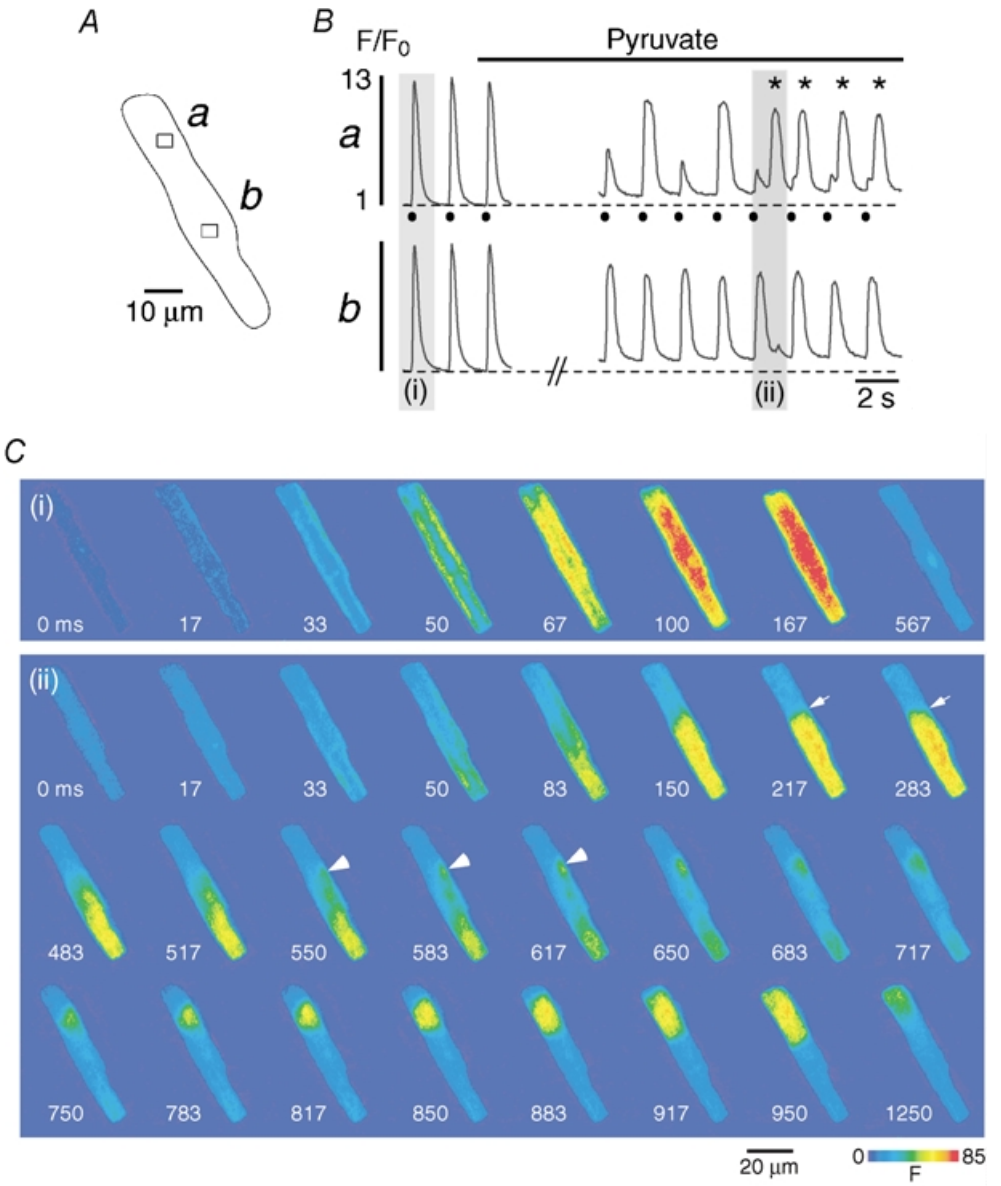

Figure 7. Subcellular Ca^{2+} alternans causes intracellular propagating Ca^{2+} waves

An atrial myocyte (*A*) is challenged with pyruvate (10 mM). *B*, subcellular $[Ca^{2+}]_i$ transients recorded from the regions *a* and *b* marked by the rectangles in *A*. *C*, cellular fluo-4 fluorescence images recorded under control conditions (i) and during pyruvate-induced Ca^{2+} alternans (ii) (shaded regions marked in *B*). 0 ms refers to the image recorded immediately preceding the first detectable increase of $[Ca^{2+}]_i$. In the presence of pyruvate region *a* exhibits Ca^{2+} alternans, whereas region *b* does not (*B*). This pattern leads to a steep $[Ca^{2+}]_i$ gradient between the two regions (*C*, panel (ii), arrows at 217 and 283 ms). A delayed localized $[Ca^{2+}]_i$ increase at the border zone (*C*, arrowheads at 550, 583 and 617 ms) gives rise to a propagating Ca^{2+} wave into the upper part of the cell (*C*, 650–1250 ms). In panel *Ba* electrical stimulations are indicated by filled circles and delayed Ca^{2+} waves are marked by asterisks. Stimulation frequency, 0.6 Hz.

two peaks (shaded area in Fig. 7*B*, panel *a*): the first peak was due to the stimulation-induced $[Ca^{2+}]_i$ increase, whereas the second was caused by the delayed Ca^{2+} wave (compare also Fig. 6*B*). Subcellular Ca^{2+} alternans could trigger repetitive Ca^{2+} waves, as shown in Fig. 7*B* (asterisks). Overall, 30 Ca^{2+} waves induced by subcellular Ca^{2+} alternans were observed in six myocytes either globally treated with pyruvate or focally challenged with pyruvate plus β-hydroxybutyrate or iodoacetate. All of these Ca^{2+} waves propagated from the region of high $[Ca^{2+}]_i$ to the region of low $[Ca^{2+}]_I$, similar to the example shown in Fig. 7*C*. The vast majority of Ca^{2+} waves (90 %, 27/30 waves) originated directly from the border zone between those two regions. Furthermore, in a given cell the origin of the Ca^{2+} waves closely followed variations in the location of the border zone during consecutive stimulations. These observations indicate that the cause of the alternans-induced Ca^{2+} waves is the steep $[Ca^{2+}]_i$ gradient between regions of high and low $[Ca^{2+}]_I$, rather than spontaneous SR Ca^{2+} release occurring randomly in a region of low $[Ca^{2+}]_i$.

DISCUSSION

Subcellular Ca^{2+} alternans and glycolysis

Previous studies on cardiac alternans were performed on multicellular cardiac preparations (e.g. whole hearts or tissue strips) or isolated cardiomyocytes, yielding valuable information on the *cellular* mechanisms of *ventricular* alternans and how ventricular alternans might lead to ventricular fibrillation and sudden cardiac death. By contrast, this is the first detailed report on the *subcellular* properties and mechanisms of Ca^{2+} alternans in *atrial* myocytes and their implications for arrhythmogenesis in the atria. Our previous investigation on electromechanical and Ca^{2+} alternans in cat atrial myocytes revealed (1) that excitation–contraction coupling and glycolysis are functionally coupled and (2) that inhibition of glycolytic flux leads to alternans (Hüser *et al.* 2000). Based on those results and the findings of others (e.g. Pierce & Philipson, 1985; Weiss & Hiltbrand, 1985; Xu *et al.* 1995), we hypothesized that the mechanisms governing cardiac alternans are regulated on a subcellularly restricted level by alterations of glycolytic flux in the microenvironment of the RyRs and/or SR Ca^{2+} pumps (Hüser *et al.* 2000). Here we provide the first *direct* evidence for this hypothesis. Our results clearly show that there are large subcellular variations in the time of onset, the magnitude and the phase of Ca^{2+} alternans within single atrial cells. Furthermore, localized metabolic inhibition through focal application of iodoacetate or pyruvate plus β-hydroxybutyrate resulted in Ca^{2+} alternans that was confined to the region of application. The localized response suggested the involvement of local metabolism, in particular glycolysis, in the modulation of SR Ca^{2+} release and the induction of Ca^{2+} alternans. Finally, we showed that subcellularly heterogeneous Ca^{2+} alternans represents a novel mechanism for the generation of propagating Ca^{2+} waves and, possibly, atrial arrhythmias.

How does inhibition of glycolysis cause Ca^{2+} alternans?

Glycolysis, although producing less than 10 % of cellular ATP, has long been recognized as the preferential energy source for membrane functions of cardiac myocytes (Weiss & Hiltbrand, 1985). Glycolytic enzymes associate with sarcolemmal and sarcoplasmic reticular membranes (Pierce & Philipson, 1985) and are functionally coupled to ion transport pathways such as the sarcolemmal K_{ATP} channel (Weiss & Lamp, 1987, 1989), the Na^+–K^+ pump (Glitsch & Tappe, 1993) and the SR Ca^{2+} pump (Xu *et al.* 1995). Thus, by controlling local pH and ATP concentration (and consequently also phosphorylation potential) in the microenvironment of sarcolemmal ion transporters, the RyR and the SR Ca^{2+} pump, glycolysis may act as a key modulator of cardiac excitation–contraction coupling. The impact of glycolysis on this process is exemplified by the demonstration that decreases of glycolytic flux result in changes in excitability (O'Rourke *et al.* 1994) and Ca^{2+} alternans (Hüser *et al.* 2000; this study), conditions known to cause arrhythmias.

Ca^{2+} alternans is due to an oscillatory change of the amount of Ca^{2+} released from the SR during an action potential. This could, in principle, be caused by three mechanisms: (1) alternations of the sarcolemmal Ca^{2+} current (I_{Ca}), i.e. the Ca^{2+} influx that triggers SR Ca^{2+} release, (2) alternations of the availability of the RyRs or (3) alternations of SR Ca^{2+} content, i.e. the amount of releasable Ca^{2+}. The latter is determined mainly by the activities of the SR Ca^{2+} pump, the RyRs and the sarcolemmal Na^+–Ca^{2+} exchange mechanism. Competition between Na^+–Ca^{2+} exchange and the SR Ca^{2+} pump for cytosolic Ca^{2+} accounts for the amount of Ca^{2+} pumped into the lumen of the SR, whereas the RyRs are responsible for the release of Ca^{2+} from the SR both during systole (Ca^{2+}-induced Ca^{2+} release; CICR) and diastole (Ca^{2+} leak). The balance between pumping and release/leak determines the SR Ca^{2+} content.

Two lines of evidence argue against alternations of I_{Ca} as a primary cause for Ca^{2+} alternans. First, Ca^{2+} alternans can be elicited during action potential clamp (Chudin *et al.* 1999), i.e. under conditions where presumably there are no beat-to-beat changes in membrane conductances, including I_{Ca}. Second, direct measurements of the Ca^{2+} current during mechanical alternans have revealed that peak I_{Ca} remains unchanged (Orchard *et al.* 1991; Hüser *et al.* 2000). Furthermore, local changes of I_{Ca} are unlikely to underlie the observed alternans patterns. If locally alternating I_{Ca} was the main cause of Ca^{2+} alternans where large parts of the cell exhibited greatly reduced Ca^{2+} release during the small amplitude $[Ca^{2+}]_i$ transient (e.g. Figs 4 and 7), then

the sum of the many local reductions of trigger Ca^{2+} would be expected to be detectable as decreased whole-cell I_{Ca}. Current evidence, however, argues against this possibility (Orchard *et al.* 1991; Hüser *et al.* 2000). It therefore appears more likely that reduced glycolytic flux mainly affects the RyRs and/or the SR Ca^{2+} pump, possibly also Na^+–Ca^{2+} exchange. Importantly, compartmentalized glycolytic ATP and/or glycolytic intermediates (Han *et al.* 1992; Xu *et al.* 1995; Kermode *et al.* 1998) seem to regulate these proteins. Ca^{2+} alternans appears to be a multi-factorial process that involves a variety of Ca^{2+} regulatory pathways. Glycolytically impaired activity of RyRs would reduce SR Ca^{2+} release and result in a small amplitude $[Ca^{2+}]_i$ transient. Consequently, less Ca^{2+} would be extruded by Na^+–Ca^{2+} exchange and more Ca^{2+} would reside in the SR. The diminished $[Ca^{2+}]_i$ transient (less Ca^{2+}-dependent inactivation) and the elevated SR Ca^{2+} content, in turn, would increase the availability of the RyRs for the next beat. Therefore, a similar amount of trigger Ca^{2+} (I_{Ca}) would now result in a large amplitude $[Ca^{2+}]_i$ transient leading to the opposite behaviour, i.e. more Ca^{2+} extrusion via Na^+–Ca^{2+} exchange, decreased SR Ca^{2+} content, and decreased availability of RyRs for the following beat (see also Eisner *et al.* 2000). Evidence from cat atrial myocytes, however, indicates that SR Ca^{2+} content (estimated as the amount of Ca^{2+} releasable by caffeine) is not different after either the small or the large amplitude $[Ca^{2+}]_i$ transient (Hüser *et al.* 2000), suggesting that alternations of SR Ca^{2+} release are quantitatively more important for metabolically induced Ca^{2+} alternans than alternations of SR Ca^{2+} content. Consistent with this idea, in rat ventricular myocytes exposed to cyanide SR Ca^{2+} release was inhibited much more strongly than SR Ca^{2+} uptake (Overend *et al.* 2001). There is indeed evidence that depression of RyR open probability can cause subcellular Ca^{2+} alternans in ventricular cells (Diaz *et al.* 2002). In addition, preliminary experiments have shown that pyruvate significantly reduces the open probability of the RyR release channel (single-channel recordings from RyRs incorporated into lipid bilayer) and the occurrence of Ca^{2+} sparks (Zima *et al.* 2002). Both these findings are additional lines of evidence that glycolysis (or its metabolites) may have a profound effect on SR Ca^{2+} release. Taken together, these results suggest that changes in the activity of the RyRs and, possibly to a smaller extent, accompanying alternations of SR Ca^{2+} content are the major mechanisms underlying cardiac Ca^{2+} alternans evoked by inhibition of glycolytic flux.

Pacing-induced Ca^{2+} alternans

Interestingly, Ca^{2+} alternans evoked by two different interventions, i.e. an increase in stimulation frequency or metabolic inhibition, had very similar characteristics suggesting the involvement of a common mechanism. During pacing-induced Ca^{2+} alternans the first small amplitude $[Ca^{2+}]_i$ transient almost always (14/15 cells) occurred when cytoplasmic $[Ca^{2+}]_i$ from the preceding transient was still elevated (Figs 1*B*, 3*B* and 4*B*). Presumably, not all of the RyRs had recovered from inactivation at this time (because of the elevated $[Ca^{2+}]_i$ and the Ca^{2+}-dependent inactivation of the RyR), so that reduced RyR activity led to a smaller $[Ca^{2+}]_i$ transient. Increased SR Ca^{2+} content and lower cytoplasmic $[Ca^{2+}]_i$ are then expected to result in a larger $[Ca^{2+}]_i$ transient for the next beat, thus creating Ca^{2+} alternans. Such a putative mechanism would be reminiscent of the mechanism proposed for Ca^{2+} alternans caused by inhibition of glycolysis. In the latter case RyR activation would be impaired because of changes in phosphorylation, local pH, and/or local ATP concentration, in the former case because of elevated $[Ca^{2+}]_i$. Alternatively, one might speculate that there are subcellular differences in local metabolism and, hence, RyR properties already under baseline conditions, and that an increase in stimulation frequency simply unmasked these differences.

Possible mechanism for the induction of arrhythmogenic Ca^{2+} waves by subcellular Ca^{2+} alternans

Commonly observed features of subcellular Ca^{2+} alternans in cat atrial myocytes were: (1) two neighbouring regions alternating out-of-phase or (2) one region displaying alternans while an adjacent region did not show any alternans. Such conditions led to steep $[Ca^{2+}]_i$ gradients between the respective subcellular regions that could cause propagating Ca^{2+} waves. Recently, a study on T-wave alternans in guinea-pig hearts revealed the mechanism linking repolarization alternans to ventricular fibrillation (Pastore *et al.* 1999). It was demonstrated that discordant alternans (i.e. neighbouring regions of the heart exhibiting out-of-phase alternans of action potential duration), if sufficient in magnitude, could cause unidirectional block and re-entry leading to ventricular fibrillation. An analogous mechanism appears to be responsible for the occurrence of the Ca^{2+} alternans-induced Ca^{2+} waves observed here. When subcellular Ca^{2+} alternans was out-of-phase ('discordant') – in analogy to electrical re-entry – 're-entry' of Ca^{2+} from the subcellular region displaying the high amplitude $[Ca^{2+}]_i$ transient into the region of low $[Ca^{2+}]_i$ generated a propagating Ca^{2+} wave. We suspect that the patterns of discordant subcellular Ca^{2+} alternans are due to a dispersion of RyR (CICR) refractoriness between neighbouring regions within a single cell, similar to the dispersion of electrical refractoriness between neighbouring cells observed at the whole heart level (Pastore *et al.* 1999). The delayed propagating Ca^{2+} wave, once triggered, is expected to cause changes of membrane potential via activation of Ca^{2+}-dependent conductances, notably the Na^+–Ca^{2+} exchange mechanism (Lipp & Pott, 1988). If sufficient in magnitude, the Ca^{2+} wave-induced after-depolarization could trigger a premature action potential and thus provide the substrate for arrhythmias (Stern *et al.*

1988; Cordeiro *et al.* 2001; Nattel, 2002). In this regard it is worth noting that, unlike most previously described Ca^{2+} waves in cardiac myocytes, the atrial Ca^{2+} waves elicited by subcellular Ca^{2+} alternans observed in the present study occurred in the apparent absence of SR Ca^{2+} overload. The amplitudes of the $[Ca^{2+}]_i$ transients during alternans were not larger than those under control conditions and there was no indication of an increase in spontaneous Ca^{2+} release events (sparks and/or waves) in between beats.

Comparison to ventricular Ca^{2+} alternans

The question arises whether similar patterns of subcellular Ca^{2+} alternans and Ca^{2+} waves can be observed in ventricular myocytes. Ventricular myocytes differ from atrial myocytes in that the latter lack a transverse (t) tubular system (McNutt & Fawcett, 1969; Hüser *et al.* 1996). This ultrastructural difference results in characteristic differences in the spatio-temporal properties of the action potential-induced $[Ca^{2+}]_i$ transient in the two types of myocyte. In ventricular myocytes, electrical stimulation elicits Ca^{2+} release simultaneously throughout the entire cell (Cheng *et al.* 1994; Berlin, 1995; Blatter *et al.* 2002). By contrast, Ca^{2+} release in atrial myocytes starts at the subsarcolemmal junctional SR before propagating to the centre of the cell via CICR from the central non-junctional SR (Berlin, 1995; Hüser *et al.* 1996; Kockskämper *et al.* 2001; Mackenzie *et al.* 2001; Blatter *et al.* 2002). The fact that SR Ca^{2+} release does not occur simultaneously in atrial myocytes and, additionally, that central release depends on subsarcolemmal release may predispose this cell type to spatial inhomogeneities in $[Ca^{2+}]_i$ during alternans, as observed in this and a previous study (Hüser *et al.* 2000). In line with this hypothesis, our recent comparison of action potential-induced $[Ca^{2+}]_i$ transients during alternans in the two cell types suggested that ventricular Ca^{2+} alternans is spatially much more homogeneous than atrial Ca^{2+} alternans (Hüser *et al.* 2000). Furthermore, in additional experiments with cat ventricular myocytes using the current imaging system we were unable to detect out-of-phase alternans and alternans-induced Ca^{2+} waves (pacing- and iodoacetate-induced Ca^{2+} alternans, $n = 11$ cells; J. Kockskämper & L. A. Blatter, unpublished observations). This finding does not rule out the possibility that, under certain conditions, substantial subcellular Ca^{2+} alternans might also occur in ventricular myocytes (e.g. Diaz *et al.* 2002). It does imply, however, that out-of-phase Ca^{2+} alternans and alternans-induced Ca^{2+} waves are much easier to induce in atrial myocytes, probably owing to their unique ultrastructure (lack of t-tubules) and the resulting spatio-temporal characteristics of SR Ca^{2+} release (Kockskämper *et al.* 2001; Mackenzie *et al.* 2001). This may also explain, in conjunction with other factors (e.g. differences in ion currents, action potential duration and refractory period between right and left atrium; see Li *et al.* 2001), why fibrillation is much more common in the atrium than in the ventricle.

In conclusion, our studies provide novel insights into the subcellular mechanisms of cardiac Ca^{2+} alternans. They implicate local metabolism, notably glycolysis, in the generation of alternans and establish a direct link between Ca^{2+} alternans and the development of Ca^{2+} waves and atrial arrhythmias.

REFERENCES

Berlin, J. R. (1995). Spatiotemporal changes of Ca^{2+} during electrically evoked contractions in atrial and ventricular cells. *American Journal of Physiology* **269**, H1165–1170.

Berlin, J. R., Cannell, M. B. & Lederer, W. J. (1989). Cellular origins of the transient inward current in cardiac myocytes. Role of fluctuations and waves of elevated intracellular calcium. *Circulation Research* **65**, 115–126.

Blatter, L. A., Sheehan, K. A. & Kockskämper, J. (2002). Subcellular calcium signalling in cardiac cells revealed with fast two-dimensional confocal imaging. *Proceedings of SPIE* **4626**, 453–463.

Cheng, H., Cannell, M. B. & Lederer, W. J. (1994). Propagation of excitation-contraction coupling into ventricular myocytes. *Pflügers Archiv* **428**, 415–417.

Cheng, H., Lederer, M. R., Lederer, W. J. & Cannell, M. B. (1996). Calcium sparks and $[Ca^{2+}]_i$ waves in cardiac myocytes. *American Journal of Physiology* **270**, C148–159.

Chudin, E., Goldhaber, J., Garfinkel, A., Weiss, J. & Kogan, B. (1999). Intracellular Ca^{2+} dynamics and the stability of ventricular tachycardia. *Biophysical Journal* **77**, 2930–2941.

Cordeiro, J. M., Bridge, J. H. B. & Spitzer, K. W. (2001). Early and delayed afterdepolarizations in rabbit heart Purkinje cells viewed by confocal microscopy. *Cell Calcium* **29**, 289–297.

Daoud, E. G., Knight, B. P., Weiss, R., Bahu, M., Paladino, W., Goyal, R., Man, K. C., Strickberger, S. A. & Morady, F. (1997). Effect of verapamil and procainamide on atrial fibrillation-induced electrical remodeling of the atria. *Circulation* **96**, 1542–1550.

Diaz, M. E., Eisner, D. A. & O'Neill, S. C. (2002). Depressed ryanodine receptor activity increases variability and duration of the systolic Ca^{2+} transient in rat ventricular myocytes. *Circulation Research* **91**, 585–593.

Eisner, D. A., Choi, H. S., Diaz, M. E., O'Neill, S. C. & Trafford, A. W. (2000). Integrative analysis of calcium cycling in cardiac muscle. *Circulation Research* **87**, 1087–1094.

Euler, D. E. (1999). Cardiac alternans: mechanisms and pathophysiological significance. *Cardiovascular Research* **42**, 583–590.

Glitsch, H. G. & Tappe, A. (1993). The Na^+/K^+ pump of cardiac Purkinje cells is preferentially fuelled by glycolytic ATP production. *Pflügers Archiv* **422**, 380–385.

Han, J. W., Thieleczek, R., Varsanyi, M. & Heilmeyer, L. M. Jr (1992). Compartmentalized ATP synthesis in skeletal muscle triads. *Biochemistry* **31**, 377–384.

Hart, R. G. & Halperin, J. L. (2001). Atrial fibrillation and stroke. Concepts and controversies. *Stroke* **32**, 803–808.

Hüser, J., Lipsius, S. L. & Blatter, L. A. (1996). Calcium gradients during excitation–contraction coupling in cat atrial myocytes. *Journal of Physiology* **494**, 641–651.

Hüser, J., Wang, Y. G., Sheehan, K. A., Cifuentes, F., Lipsius S. L. & Blatter, L. A. (2000). Functional coupling between glycolysis and excitation–contraction coupling underlies alternans in cat heart cells. *Journal of Physiology* **524**, 795–806.

Kermode, H., Chan, W. M., Williams, A. J. & Sitsapesan, R. (1998). Glycolytic pathway intermediates activate cardiac ryanodine receptors. *FEBS Letters* **431**, 59–62.

Kockskämper, J., Sheehan, K. A., Bare, D. J., Lipsius, S. L., Mignery, G. A. & Blatter, L. A. (2001). Activation and propagation of Ca^{2+} release during excitation–contraction coupling in atrial myocytes. *Biophysical Journal* **81**, 2590–2605.

Levy, S. (1998). Epidemiology and classification of atrial fibrillation. *Journal of Cardiovascular Electrophysiology* **9**, S78–82.

Li, D., Zhang, L., Kneller, J. & Nattel, S. (2001). Potential ionic mechanism for repolarization differences between canine right and left atrium. *Circulation Research* **88**, 1168–1175.

Lipp, P. & Pott, L. (1988). Transient inward current in guinea-pig atrial myocytes reflects a change of sodium–calcium exchange current. *Journal of Physiology* **397**, 601–630.

Mackenzie, L., Bootman, M. D., Berridge, M. J. & Lipp, P. (2001). Predetermined recruitment of calcium release sites underlies excitation–contraction coupling in rat atrial myocytes. *Journal of Physiology* **530**, 417–429.

McNutt, N. S. & Fawcett, D. W. (1969). The ultrastructure of the cat myocardium. II. Atrial muscle. *Journal of Cell Biology* **42**, 46–67.

Nattel, S. (2002). New ideas about atrial fibrillation 50 years on. *Nature* **415**, 219–226.

Nattel, S., Li, D. & Yue, L. (2000). Basic mechanisms of atrial fibrillation – very new insights into very old ideas. *Annual Review of Physiology* **62**, 51–77.

Newsholme, E. A., Randle, P. J. & Manchester, K. L. (1962). Inhibition of the phosphofructokinase reaction in the perfused rat heart by respiration of ketone bodies, fatty acids and pyruvate. *Nature* **193**, 270–271.

Orchard, C. H., McCall, E., Kirby, M. S. & Boyett, M. R. (1991). Mechanical alternans during acidosis in ferret heart muscle. *Circulation Research* **68**, 69–76.

O'Rourke, B., Ramza, B. M. & Marban, E. (1994). Oscillations of membrane current and excitability driven by metabolic oscillations in heart cells. *Science* **265**, 962–966.

Overend, C. L., Eisner, D. A. & O'Neill, S. C. (2001). Altered cardiac sarcoplasmic reticulum function of intact myocytes of rat ventricle during metabolic inhibition. *Circulation Research* **88**, 181–187.

Pastore, J. M., Girouard, S. D., Laurita, K. R., Akar, F. G. & Rosenbaum, D. S. (1999). Mechanism linking T-wave alternans to the genesis of cardiac fibrillation. *Circulation* **99**, 1385–1394.

Pierce, G. N. & Philipson, K. D. (1985). Binding of glycolytic enzymes to cardiac sarcolemmal and sarcoplasmic reticular membranes. *Journal of Biological Chemistry* **260**, 6862–6870.

Rubenstein, D. S. & Lipsius, S. L. (1995). Premature beats elicit a phase reversal of mechanoelectrical alternans in cat ventricular myocytes. *Circulation* **91**, 201–214.

Shimizu, W. & Antzelevitch, C. (1999). Cellular and ionic basis for T-wave alternans under long-QT conditions. *Circulation* **99**, 1499–1507.

Smith, J. M., Clancy, E. A., Valeri, C. R., Ruskin, J. N. & Cohen, R. J. (1988). Electrical alternans and cardiac electrical instability. *Circulation* **77**, 110–121.

Stern, M. D., Capogrossi, M. C. & Lakatta, E. G. (1988). Spontaneous calcium release from the sarcoplasmic reticulum in myocardial cells: mechanisms and consequences. *Cell Calcium* **9**, 247–256.

Tieleman, R. G., De Langen, C., Van Gelder, I. C., De Kam, P. J., Grandjean, J., Bel, K. J., Wijffels, M. C., Allessie, M. A. & Crijns, H. J. (1997). Verapamil reduces tachycardia-induced electrical remodeling of the atria. *Circulation* **95**, 1945–1953.

Trafford, A. W., Lipp, P., O'Neill, S. C., Niggli, E. & Eisner, D. A. (1995). Propagating calcium waves initiated by local caffeine application in rat ventricular myocytes. *Journal of Physiology* **489**, 319–326.

Trafford, A. W., O'Neill, S. C. & Eisner, D. A. (1993). Factors affecting the propagation of locally activated systolic Ca transients in rat ventricular myocytes. *Pflügers Archiv* **425**, 181–183.

Van Wagoner, D. R., Pond, A. L., Lamorgese, M., Rossie, S. S., McCarthy, P. M. & Nerbonne, J. M. (1999). Atrial L-type Ca^{2+} currents and human atrial fibrillation. *Circulation Research* **85**, 428–436.

Verrier, R. L. & Nearing, B. D. (1994). Electrophysiologic basis for T wave alternans as an index of vulnerability to ventricular fibrillation. *Journal of Cardiovascular Electrophysiology* **5**, 445–461.

Weiss, J. & Hiltbrand, B. (1985). Functional compartmentation of glycolytic *versus* oxidative metabolism in isolated rabbit heart. *Journal of Clinical Investigation* **75**, 436–447.

Weiss, J. N. & Lamp, S. T. (1987). Glycolysis preferentially inhibits ATP-sensitive K^+ channels in isolated guinea pig cardiac myocytes. *Science* **238**, 67–69.

Weiss, J. N. & Lamp, S. T. (1989). Cardiac ATP-sensitive K^+ channels: evidence for preferential regulation by glycolysis. *Journal of General Physiology* **94**, 911–935.

Wier, W. G. & Blatter, L. A. (1991). Ca^{2+}-oscillations and Ca^{2+}-waves in mammalian cardiac and vascular smooth muscle cells. *Cell Calcium* **12**, 241–254.

Wohlfart, B. (1982). Analysis of mechanical alternans in rabbit papillary muscle. *Acta Physiologica Scandinavica* **115**, 405–414.

Wu, J., Vereecke, J., Carmeliet, E. & Lipsius, S. L. (1991). Ionic currents activated during hyperpolarization of single right atrial myocytes from cat heart. *Circulation Research* **68**, 1059–1069.

Wu, Y. & Clusin, W. T. (1997). Calcium transient alternans in blood-perfused ischemic hearts: observations with fluorescent indicator Fura Red. *American Journal of Physiology* **273**, H2161–2169.

Xu, K. Y., Zweier, J. L. & Becker, L. C. (1995). Functional coupling between glycolysis and sarcoplasmic reticulum Ca^{2+} transport. *Circulation Research* **77**, 88–97.

Zima, A., Kockskämper, J. & Blatter, L. A. (2002). Pyruvate-mediated effects on cardiac Ca^{2+} signaling. *Biophysical Journal* **82**, 71a.

Acknowledgements

The authors thank Drs S. L. Lipsius and A. M. Samarel for insightful discussions and comments on the manuscript. This work was supported by the NIH (HL62231 to L.A.B.) and fellowships from the Falk Foundation (Loyola University Chicago) and the Deutsche Forschungsgemeinschaft (DFG) to J.K. The expert technical assistance of Holly Gray is gratefully acknowledged.

Author's present address

J. Kockskämper: Abteilung Kardiologie und Pneumologie, Georg-August-Universität, Robert-Koch-Str. 40, 37075 Göttingen, Germany.